Gold Nanoparticles Synthesized via Pulsed Laser Ablation: Physical and Biological Characterization

Sabah Anwer Salman[1], Salma Salman Abdullah[2], Waleed Hatem Namous[2] and Faisal Laith Ahmed[2]
[1]*Department of Physics, College of Science, University of Diyala, 32001 Baquba, Iraq*
[2]*General Directorate for Education of Diyala,32001 Baqubah, Iraq*
pro.dr_sabahanwer@yahoo.com, {dr.salmaalshamari, waleedalnidawy989, faisalstar} @gmail.com

Keywords: Gold, Nanoparticles, Syzygium Aromaticum, Laser Ablation, S. Aureus, K. Pneumonia, P. Aeruginosa, A. Baumannii.

Abstract: Gold nanoparticles (AuNPs) were produced via pulsed laser ablation using a *syzygium aromaticum* solution. The varying pulse rates employed were 500, 750, and 1000, with an extract in which eugenol serves as a reducing agent. The synthesized AuNPs were analyzed using ED-XRF, XRD, UV–VIS spectroscopy, and Transmission electron microscopy TEM. ED-XRF analysis revealed that the utilized gold alloy exhibited a high purity of approximately 98.66%. XRD studies showed that the gold nanoparticles feature a face-centered cubic (FCC) crystal structure, with a predominant crystalline orientation of (111). The optical analysis of samples was conducted using a UV-VIS spectrophotometer, which indicated a surface plasmon resonance (SPR) peak at a wavelength of 520 nm. Additionally, the energy gap values increased to 2.05 eV for AuNPs and 2.73 eV for S. aromaticum. TEM images confirmed the presence of nanoparticles at the nanoscale. Biological activity showed a weak effect of nano-solutions on bacterial species (S. aureus, K. pneumonia, P. aeruginosa and A. baumannii).

1 INTRODUCTION

Over the past five decades, nanotechnology has experienced exponential growth and revolutionized a variety of industrial applications [1]. Environmental science, agriculture, food technology, biotechnology, biomedicine, and pharmaceuticals are just a few of the fields that could be profoundly affected by developments in this domain, which deals with components with dimensions ranging from 1 to 100 nm [2], [3]. Metal nanoparticles (NPs) have considerable potential because their optical, electronic, and catalytic properties are better than those of bulk materials [4]. Gold nanoparticles (AuNPs) are very popular compared to other metallic nanoparticles because they are easy to make and offer many advantages in medicine, like treating diabetes, cancer, heart diseases, tuberculosis, and helping with antibiotic resistance [5], [6]. Additionally, AuNPs have powerful and long-lasting antioxidant properties, making them effective against free radicals and Reactive Oxygen Species which are linked to many degenerative diseases [7]. As a consequence of the interaction between electromagnetic waves and confined electron gas, noble metal nanoparticles exhibit surface plasmon resonance (SPR) optical properties that depend on their shape and size. The catalytic, biosensing, bioimaging, cancer therapy, and drug delivery capacities of AgNPs and AuNPs are worth investigating further [8], [9]. There is a large amount of research that looks at the green synthesis of AgNPs and AuNPs employing bacteria, fungi, and plant extracts as reducing agents [8]-[14]. Scientists have documented the use of extracts from various fruits, including pomegranate, blackberry, blueberry, Emblica officinalis, turmeric, and Garcinia indica. As shown in Figure 1 Various synthesis approaches of AuNPs [15].

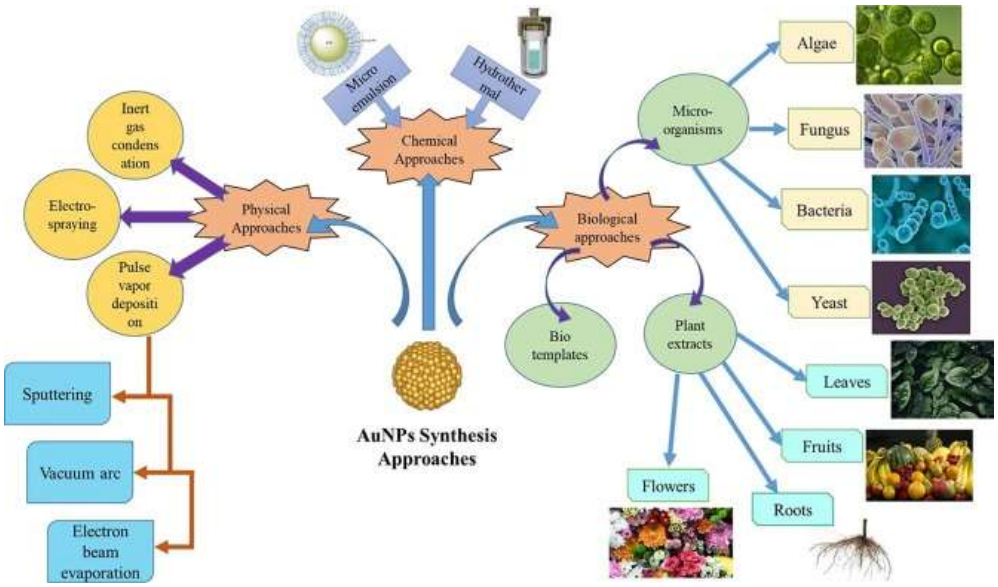

Figure 1: Various synthesis approaches of AuNPs [15].

The dried flower bud, which is also called clove, is a member of the Myrtaceae family. It was originally from the Maluku Islands in Indonesia but is now grown all over the world. Commercially valuable components of clove trees are their buds and leaves; four years after planting, the tree begins to produce flowering buds. The next step is to harvest them before they bloom, either by hand or with the help of a natural phytohormone [16], [17]. There are a number of medicinal and aromatic uses for cloves in business settings. Because of their antioxidant and antibacterial qualities, these spices are thought of as a natural alternative to artificial preservatives in many different types of food, particularly when it comes to processing meat [16], [18]. Cinnamon, oregano, clove, thyme, and mint are fragrant herbs that have antimicrobial, antiviral, anticarcinogenic, and antifungal properties, according to multiple studies. Due to its exceptional antibacterial and antioxidant properties, clove has become a prominent spice [19]-[22]. In recent years, researchers have synthesized gold nanoparticles from Syzygium aromaticum extract and used them to enhance the response of a colorimetric urea sensor. This study showed that the particles have polygonal and triangular shapes, ranging in size from 4 to 150 nanometers. [23]. They have also studied the characterization and antioxidant activity of gold nanoparticles from carnation flower water extract, the research found the AuNPs has a maximum wavelength at 533 nm, and particle size of 73.52 nm [24]. As shown in Figure 2 S. aromaticum and its uses in biological activities [25].

Figure 2: *S.* aromaticum and its uses in biological activities [25].

2 MATERIALS AND METHODOLOGY

A highly pure Au plate has purity of (98.66%), this target was cleaned using an acetone solvent in the ultrasonic bath for (15 minutes), was cleaned in an ultrasonic bath for (15 minutes) with an acetone solvent, then washed with ethanol and deionized distilled water (DDW) to remove the organic pollutants. To prepare the clove stick extract, clove sticks were purchased from a local company. The sticks were cleaned and washed with DDW. Then,

they were transferred to a 100-ml beaker, mixed with 80 ml of deionized water, and agitated at 40°C for 1 hour. The extract solution was filtered using filter paper, placed on a magnetic stirrer for an additional hour, cooled, and subsequently transferred to tubes for further purification. A pulsed Nd:YAG laser (λ= 1064 nm, E= 500 mJ, pulse duration 10 ns, repetition rate 1 Hz and he pulse counts were (500,750, and 1000)) served as the radiation source for the ablation process.

The distance from the target to the lens was 7 cm. The beaker was placed on a rotating device to aim the laser beam at the target for nanoparticle ablation. The solution's color change was observed after each pulse count. The diameter of the laser beam on the metallic surface was measured at 2 mm.

The nanoparticles were synthesized using pulsed laser ablation of a gold alloy. The gold was positioned as a target at the bottom of a glass beaker holding 2ml of S. aromaticum solution.

ED-XRF spectroscopy made in Germany (type XEPOS). XRD utilizing a Lab-X (XRD-6000) Shimadzu diffractometer from Japan. Absorption spectra and Surface Plasmon Resonance (SPR) were obtained for colloids utilizing a Double Beam 1800 UV Spectrometer produced by Shimadzu, Japan, to ascertain effective aggregates. Transmission electron microscopy examinations were performed using a ZEISS LED 912 AB-100KV apparatus from Germany. Mueller-Hinton agar was formulated by dissolving 38 grams in one liter of distilled water, sterilizing the solution in an autoclave at 121°C and 15 pounds for 15 minutes, thereafter, cooling it, dispensing it onto sterile plates, and refrigerating it until required. The antibacterial effect of the formulated solutions was assessed utilizing the agar well diffusion technique. A series of bacterial colonies were transferred with a loop to prepare the suspended bacteria, which were subsequently introduced into tubes containing brain broth for activation. The tubes were incubated at 37°C for a duration of 18 to 24 hours. The suspended bacteria were evaluated against a standard McFarland solution comprising 1.5 × 108 cells/ml. The bacterial suspension was thereafter applied with a sterile swab onto Mueller-Hinton agar plates and permitted to dry. Holes were formed in the culture medium with a sterile cork punch, and 100 µL of the material was individually dispensed into each hole using a micropipette (100, 75, 50 and 25) in each well. The efficacy of each concentration was assessed by measuring the diameter of the inhibitory zone around each aperture.

3 RESULTS AND DISCUSSION

3.1 ED-XRF Results

The makeup of elements and the purity of metal used before the pulsed laser ablation in liquids were checked with (ED-XRF), showing about 98.66% purity for the gold plate. Figure 3 illustrate this.

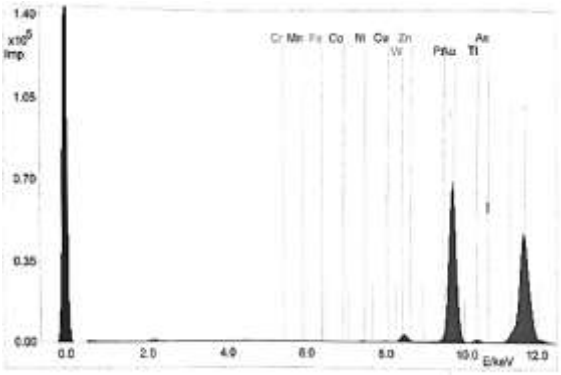

Figure 3: X-ray fluorescence spectrum of gold metal.

3.2 XRD Results

Figure 4 depicts the outcomes of the thorough characterization of the sample data. X-ray diffraction characterization was conducted on the sample (AuNPs). The Debye–Scherrer (1) was employed to assess the crystalline size (D) of the synthesized Au nanoparticles [26]:

$$D = \frac{K\lambda}{\beta \cos\theta}, \quad (1)$$

where:

- k: is shape factor;
- λ: is the wavelength of incident x-ray radiation = (1.5406 Å for CuKα);
- β: is the full width at half maximum (FWHM) of the peak (in radians);
- θ: is Bragg's angle.

The X-ray diffraction results of a gold nanoparticle solution produced in (DDW) and placed on a quartz slide measuring (1 cm x 1 cm) indicated that the crystal structure is cubic. Figure 4 reveals four peaks at angles (38.23°, 44.68°, 64.72°, 77.61°), corresponding to the indices (111), (200), (220), and (311). These findings align closely with the values specified in ICDD card no. (00-001-1172) for gold. The crystal plane orientation (111) is predominant. Table 1 illustrates the concordance between the standard and experimental data, exhibiting a minor deviation in the distances of the atomic planes (d).

The lattice strain caused by imperfections influences the preparation of nanomaterials [27]. Laser power is the most important factor affecting the properties, size, and concentration of the extracted metal nanoparticles. The solution was observed to be discolored after several laser pulses. In the absorption spectra of the solutions, the surface plasmon peak could be clearly distinguished, ranging between 520 nm, which is consistent with the results XRD in the presence of small particles with wavelengths ranging from 3 to 30 nm in the solution, as shown in Table 1 [28].

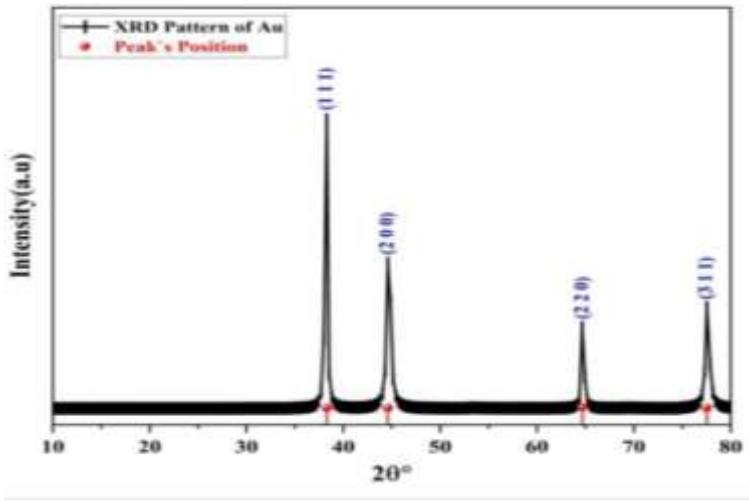

Figure 4: X-ray diffraction pattern of Au nanoparticles prepared by laser ablation method.

Table 1: Structural properties of Au NPs.

2θ (deg) Experimental	2θ (deg) Standard	FWHM (deg)	(hkl)	dhkl (Å) Experimental	dhkl (Å) Standard	D(nm)
38.23	38.26	0.3361	111	2.355	2.350	25.05
44.68	44.60	0.5538	200	2.027	2.030	15.53
64.72	64.67	0.3730	220	1.439	1.440	25.24
77.61	77.54	0.4935	311	1.230	1.230	20.67

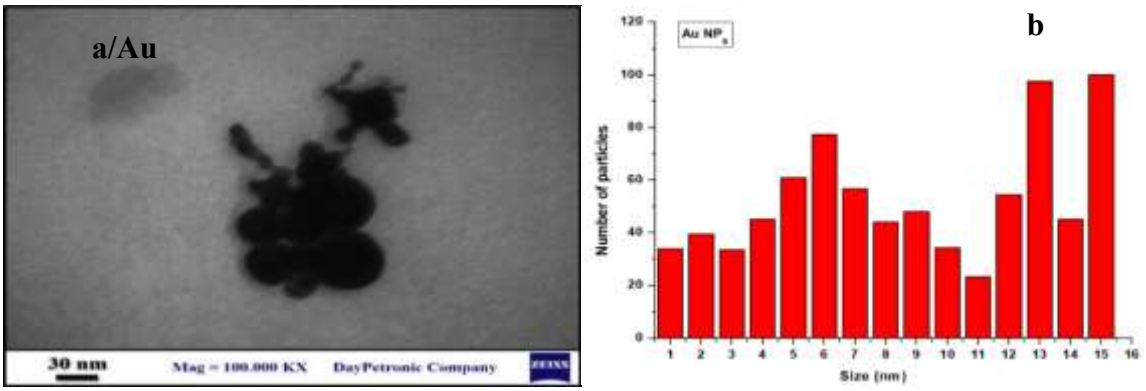

Figure 5: TEM characterization of AuNPs prepared in DDW: a) TEM image and b) particle size distribution.

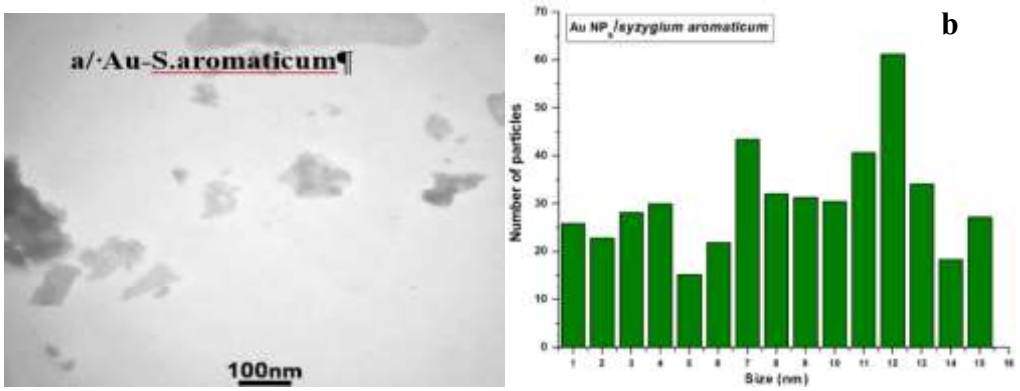

Figure 6: TEM characterization of Au/syzygium aromaticum nanoparticles: a) TEM image and b) particle size distribution.

3.3 TEM Results

Figures 5 and 6 present the TEM micrographs and particle size distributions of AuNPs and Au/syzygium aromaticum nanoparticles synthesized in DDW. The TEM images reveal that the prepared nanoparticles exhibit predominantly spherical and slightly irregular morphologies. In addition, a noticeable reduction in particle size was observed after the incorporation of syzygium aromaticum extract.

The TEM images were recorded at magnifications of 100,000× with scale bars of 30 nm and 100 nm. The particle size analysis was carried out using ImageJ software, while the statistical size distribution histograms were generated using OriginPro 8.5 software.

The average particle sizes were estimated to be approximately 53.05 nm for pure AuNPs and 30.88 nm for Au/syzygium aromaticum nanoparticles. The reduction in nanoparticle size indicates the significant role of the plant extract in controlling nanoparticle growth and improving particle dispersion.

3.4 Optical Properties Results

Since the absorption band grows in direct proportion to the size and aspect ratio of nanoparticles, absorption spectroscopy was used to examine their optical characteristics. Figure 7 depicts the UV-VIS spectrum of fluorescent solutions created from pulsed laser ablation of gold plates in (DDW) solutions, respectively. The location of the surface plasmon peak at approximately 520 nm and the absorbance (0.386) of the gold nanoparticles are shown in Figure 6. These parameters indicate the generation of the nanoparticles and can be explained by the absorption generated by the interband transition in the nanoparticles. It is possible that electrons in noble metals undergo interband absorption at shorter wavelengths as a result of their transition from the occupied d-level state to the unoccupied state in the conduction band above the Fermi level [29]. It had a lower peak intensity than deionized water, indicating an increase in gold (Au) nanoparticle manufacturing efficiency [30]. spectra can determine the energy gap of the Au nanoparticles using Tauc's formula [31]:

$$(\alpha h\upsilon)^n = B\,(h\upsilon - Eg). \quad (2)$$

B: is a constant, hυ: the photon energy, h: Plank's constant, ν: photon's frequency, n: a value of 2 or 1/2, α: the absorption coefficient. Calculated from the measured absorbance (A) at the wavelength of light (λ) using [31]:

$$A = -\log 10T. \quad (3)$$

Figure 7 illustrates that the optical energy gap edge of the synthesized nanoparticles increases at 500, 750, and 1000 pulses in comparison to the optical energy gap of deionized distilled water and Syzygium aromaticum. The alteration in the energy gap edge can be attributed to the decrease in nanoparticle size resulting from quantum confinement. Thus, a larger energy gap value facilitates the uptake of small-sized particles [31]. Table 2 shows the absorption and energy gap values of colloidal samples.

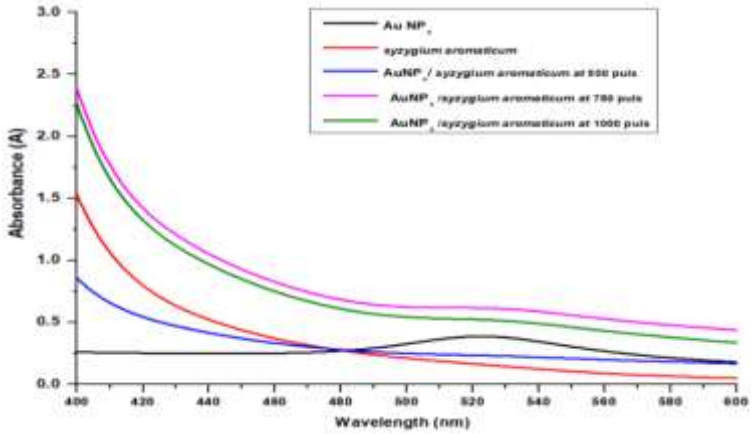

Figure 7: UV-Visible absorption spectra of colloidal Au nanoparticles and Au/ /syzygium aromaticum.

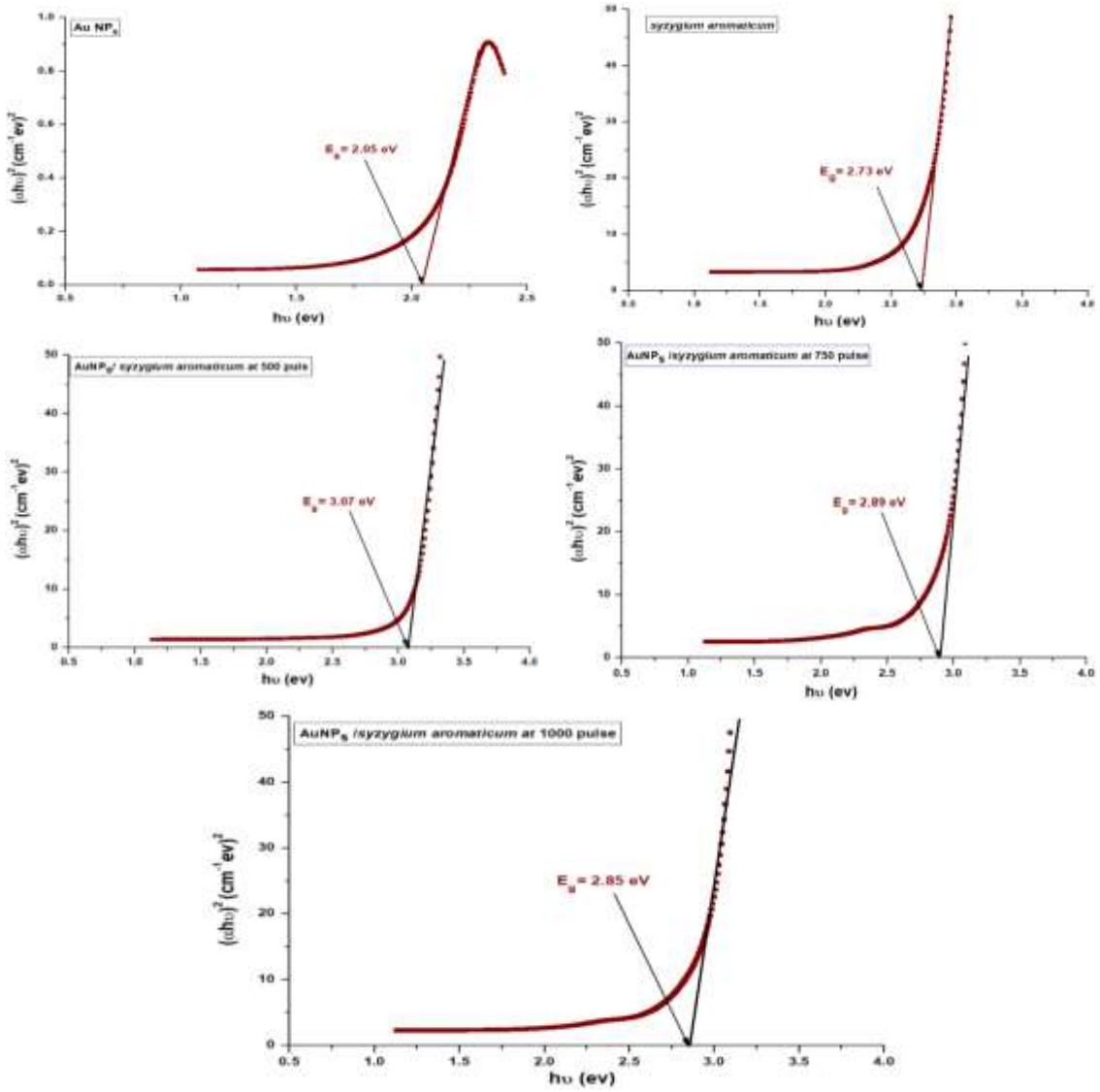

Figure 8: Direct band gap estimations of colloidal samples.

Table 2: The absorption and energy gap values of colloidal samples.

Liquid	Absorbance (a. u)	Eg (eV)
AuNPs	0.386	2.05
Syzygium aromaticum	1.53	2.73
AuNPs/ syzygium aromaticum at 500 pulse	0.843	3.07
AuNPs/ syzygium aromaticum at 750 pulse	2.393	2.89
AuNPs/ syzygium aromaticum at 1000 pulse	2.258	2.85

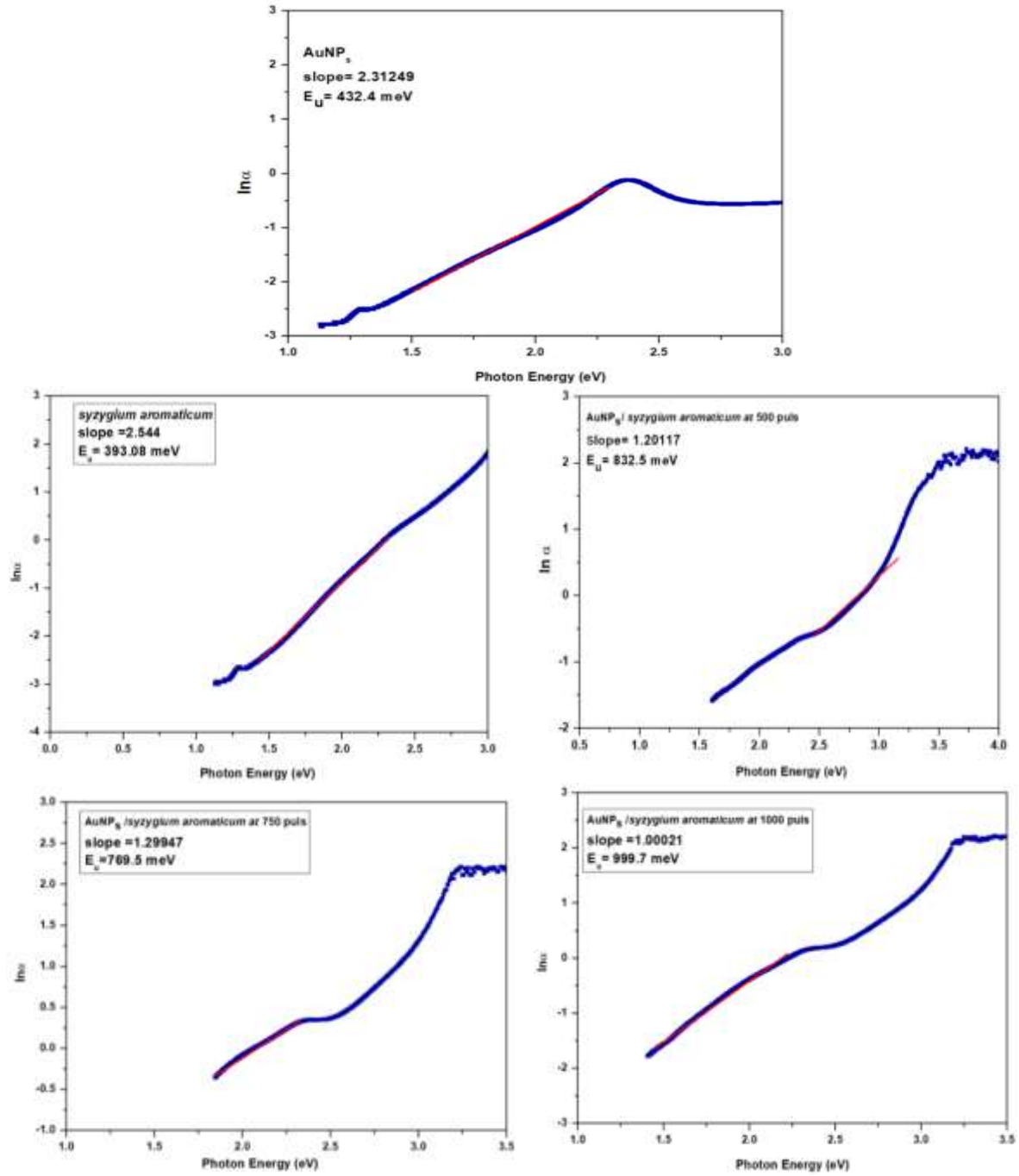

Figure 9: Urbach energy estimations of colloidal samples.

Table 3: The inhibition zone diameter (mm) of types of bacteria at different concentrations of Au/S.armaticum.

Concentration	*S. aureus*	*K. pneumonia*	*P. aeruginosa*	*A. baumannii*
Control	0 mm	0 mm	0 mm	0 mm
25	0 mm	0 mm	0 mm	0 mm
50	0 mm	0 mm	0 mm	0 mm
75	12 mm	10 mm	0 mm	11 mm
100	13 mm	11mm	10 mm	18 mm

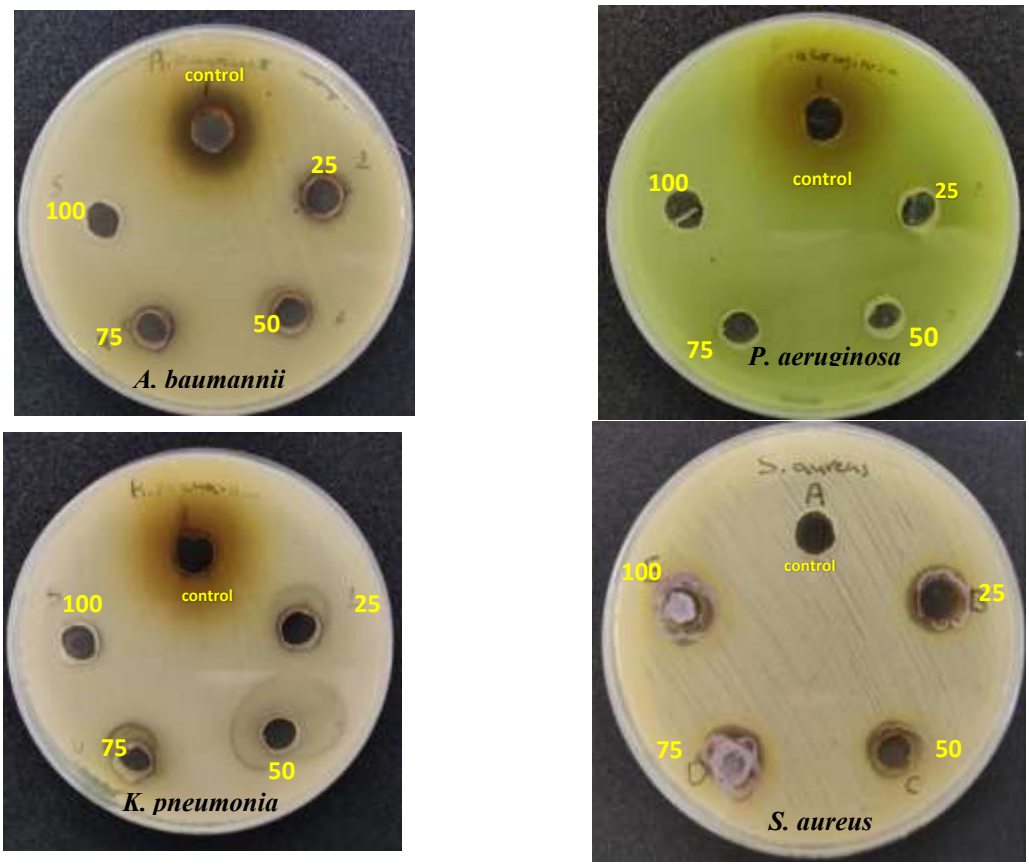

Figure 10: Inhibition zone (mm) of colloidal samples.

3.4.1 Urbach Energy

The Urbach energy (E_u) was determined utilizing equation [32]:

$$\alpha = \alpha_{\circ} exp(\frac{h\vartheta}{E_u}) . \quad (3)$$

Where:

- α: is absorption coefficient;
- αo: is constant;
- hυ: is the photon energy;
- Eu: is Urbach energy.

Figure 9 depicts the correlation between (lnα) and photon energy (hυ). The Urbach energy denotes the breadth of the permitted localized states within the energy gap and is determined by the inverse of the linear segment's slope in the exponential region. The Urbach energy value rises with an increasing weight ratio. The way Urbach energy behaves with light is different from how the energy gap behaves, because when Urbach energy increases, it means the localized levels within the energy gap are getting wider. This outcome aligns with the prior study [30].

3.5 Bioactivity Test

Clove oil, in its natural form, contains ß-caryophyllene, tannins, and phenols; it is derived from the blossom buds of S. aromaticum. One of the most important components of the oil is eugenol,

which gives the plant its signature aroma. Clove oil has a long list of traditional purposes, and several scientific investigations have highlighted these benefits, highlighting its antioxidant, hypotensive, antibacterial, anti-inflammatory, and antifungal properties [33], [34]. The advent of multidrug-resistant bacteria has increased the prevalence of infectious diseases globally. Consequently, the advancement of antimicrobial agents is vital due to the increasing burden of multidrug-resistant bacteria originating from food. Gold nanoparticles have demonstrated considerable antibacterial efficacy against Gram-negative microorganisms in food. Consequently, AuNPs may serve as an effective alternative for developing drugs against multidrug-resistant bacterial strains. The functions of AuNPs may lead to significant discoveries across various domains [35]. Figure 10 showed that the antibacterial activity of (Au/ S. aromaticum) nanoparticles from (S. aureus) was the highest among the other microorganisms. The results indicated that the antibacterial activity varied depending on the target bacteria, including A. baumannii, P. aeruginosa, Klebsiella pneumoniae, and S. aureus. Notably, all bacteria showed sensitivity to the Au/S. aromaticum nanoparticle solution at high concentrations only Comparing the relative inhibition zone, the antibacterial activity of the Au/S. aromaticum nanoparticles against Staphylococcus aureus was the highest among the other bacteria. These gold nanoparticles exhibited antibacterial activity and had inhibition zones of 13 and 16 mm for S. aureus and A. baumannii, respectively.as shown in Table 3. These results are consistent with previous studies [36].

4 CONCLUSIONS

In conclusion, this study illustrated the effective utilisation of an aqueous extract of S. aromaticum flowers in the manufacture of gold nanoparticles using pulsed laser ablation at a maximum wavelength of 1064 nm, employing different pulse counts (500, 750, and 1000), hence indicating their potential biomedical applications. X-ray diffraction (XRD) examination of the synthesised gold nanoparticles validated a face-centered cubic (FCC) crystal structure. Additionally, transmission electron microscopy (TEM) research demonstrated that the nanoparticles were spherical, predominantly composed of gold, and measured 30.88 nm in diameter, whereas (Au/S.aromaticum) exhibited dimensions of 53.05 nm. The nanoparticle structure was additionally validated by UV-VIS spectroscopy. These gold nanoparticles exhibited antibacterial activity, with inhibition zones of 13 and 16 mm for Staphylococcus aureus and A. baumannii, respectively. This study highlighted the potential of environmentally friendly preparation methods in improving the physical and chemical properties of manufactured nanoparticles and medicinal herb extracts, for use in biomedical applications.

ACKNOWLEDGMENTS

The authors would like to express their sincere gratitude to the Department of Physics, College of Science, University of Diyala, for their continuous support and provision of the necessary facilities to conduct this research.

REFERENCES

[1] S. A. Afolalu, J. F. Kayode, S. I. Monye, S. L. Lawal, and O. M. Ikumapayi, “An overview of nanotechnology and its application,” E3S Web of Conferences, vol. 391, pp. 1-17, 2023, [Online]. Available: https://doi.org/10.1051/e3sconf/202339101079.

[2] K. A. Al Tammar, “A review on nanoparticles: characteristics, synthesis, applications, and challenges,” Front. Microbiol., vol. 14, p. 1155622, 2023, [Online]. Available: https://doi.org/10.3389/fmicb.2023.1155622.

[3] K. K. Bharadwaj, B. Rabha, S. Pati, T. Sarkar, B. K. Choudhury, A. Barman, and N. H. Noor, “Green synthesis of gold nanoparticles using plant extracts as beneficial prospect for cancer theranostics,” Molecules, vol. 26, pp. 63-89, 2021, [Online]. Available: https://doi.org/10.3390/molecules26010063.

[4] S. A. Salman, N. A. Bakr, and S. S. Abduallah, “Study of thermal decomposition and FTIR for PVA–AlCl composite films,” J. Eng. Appl. Sci., vol. 14, pp. 717-724, 2019, [Online]. Available: https://doi.org/10.3923/jeasci.2019.717.724.

[5] T. M. S. Erlangga, A. B. D. Nandiyanto, and M. Fiandini, “Analysis technoeconomic pada produces nanoparticle Emma’s (AuNP) Degnan method biosynthesis manganoan Sargassum horneri pada skala industry,” J. Teknik Ind., vol. 1, pp. 103-110, 2020.

[6] D. N. Sari and T. Taufikurohmah, “Pengaruh penambahan nanogold terhadap aktivitas antioksidan ekstrak gambir (Uncaria gambir Roxb.),” UNESA J. Chem., vol. 8, pp. 1-10, 2019.

[7] M. H. Ibroham, S. Jamilatun, and I. D. Kumalasari, “A review: Potensi tumbuhan-tumbuhan di Indonesia sebagai antioksidan alami,” in Seminar Nasional Penelitian LPPM UMJ, vol. 1, pp. 1-13, 2022.

[8] K. S. Kavitha, S. Baker, D. Rakshith, H. U. Kavitha, H. C. Y. Rao, B. P. Harini, and S. Satish, "Plants as green source towards synthesis of nanoparticles," Int. Res. J. Biol. Sci., vol. 2, pp. 66-76, 2013.

[9] V. Vadlapudi, D. S. V. G. K. Kaladhar, M. Behara, G. K. Naidu, and B. Sujatha, "Review: Green synthesis of silver and gold nanoparticles," Int. J. Chem. Stud., vol. 1, pp. 22-31, 2013.

[10] S. S. Shankar, A. Rai, A. Ahmad, and M. Sastry, "Controlling the optical properties of lemongrass extract synthesized gold nanotriangles and potential application in infrared absorbing coatings," Chem. Mater., vol. 17, no. 3, pp. 566-572, 2005, [Online]. Available: https://doi.org/10.1021/cm048128q.

[11] B. Ankamwar, C. Damle, A. Ahmad, and M. Sastry, "Biosynthesis of gold and silver nanoparticles using Emblica officinalis fruit extract, their phase transfer and transmetallation in an organic solution," J. Nanosci. Nanotechnol., vol. 5, pp. 1665-1671, 2005, [Online]. Available: https://doi.org/10.1166/jnn.2005.352.

[12] R. S. R. Isaac, G. Saktivel, and Ch. Murthy, "Green synthesis of gold and silver nanoparticles using Averrhoa bilimbi fruit extract," J. Nanotechnol., vol. 2013, pp. 1-6, 2013, [Online]. Available: https://doi.org/10.1155/2013/927870.

[13] M. N. Nadagouda, N. Iyanna, J. Lalley, C. Han, D. D. Dionysiou, and R. S. Varma, "Synthesis of silver and gold nanoparticles using antioxidants from blackberry, blueberry, pomegranate and turmeric extracts," ACS Sustain. Chem. Eng., vol. 2, pp. 1717-1723, 2014, [Online]. Available: https://doi.org/10.1021/sc500194s.

[14] M. Krishnaprabha and M. Pattabi, "Synthesis of gold nanostructures using fruit extract of Garcinia indica," AIP Conf. Proc., vol. 1731, p. 050122, 2016, [Online]. Available: https://doi.org/10.1063/1.4947754.

[15] M. A. Khan, M. S. Al Mamun, M. A. Habib, A. B. M. N. Islam, K. M. R. Karim, J. Naime, P. Saha, and M. H. Ara, "A review on gold nanoparticles: Biological synthesis, characterizations, and analytical applications," Results Chem., vol. 4, p. 100478, 2022, [Online]. Available: https://doi.org/10.1016/j.reschm.2022.100478.

[16] D. F. Cortés-Rojas, C. R. de Souza, and W. P. Oliveira, "Clove (Syzygium aromaticum): A precious spice," Asian Pac. J. Trop. Med., vol. 4, pp. 90-96, 2014, [Online]. Available: https://doi.org/10.1016/S1995-7645(14)60003-9.

[17] G. E. S. Batiha, A. A. Beshbishy, D. S. Tayebwa, M. H. Shaheen, N. Yokoyama, and I. Igarashi, "Inhibitory effects of Syzygium aromaticum and Camellia sinensis methanolic extracts on the growth of Babesia and Theileria parasites," Ticks Tick-Borne Dis., vol. 10, pp. 949-958, 2019, [Online]. Available: https://doi.org/10.1016/j.ttbdis.2019.05.004.

[18] N. Chomchalow, "Spice production in Asia-An overview," in Proc. IBC's Asia Spice Markets 96 Conf., Singapore, pp. 27-28, 1996.

[19] B. Shan, Y. Z. Cai, M. Sun, and H. Corke, "Antioxidant capacity of 26 spice extracts and characterization of their phenolic constituents," J. Agric. Food Chem., vol. 53, pp. 7749-7759, 2005, [Online]. Available: https://doi.org/10.1021/jf051513e.

[20] F. B. Hu and W. C. Willett, "Optimal diets for prevention of coronary heart disease," JAMA, vol. 288, pp. 2569-2578, 2002, [Online]. Available: https://doi.org/10.1001/jama.288.20.2569.

[21] R. I. Astuti, S. Listyowati, and W. T. Wahyuni, "Life span extension of model yeast Saccharomyces cerevisiae upon ethanol-derived clover bud extract treatment," IOP Conf. Ser. Earth Environ. Sci., vol. 299, p. 012059, 2019, [Online]. Available: https://doi.org/10.1088/1755-1315/299/1/012059.

[22] N. Sarrami, M. Pemberton, M. Thornhill, and E. D. Theaker, "Adverse reactions associated with the use of eugenol in dentistry," Br. Dent. J., vol. 193, pp. 249-253, 2002, [Online]. Available: https://doi.org/10.1038/sj.bdj.4801701.

[23] K. Baljit, M. Minakshi, and M. Minni, "Green synthesis of gold nanoparticles from Syzygium aromaticum extract and its use in enhancing the response of a colorimetric urea biosensor," BionanoScience, vol. 2, pp. 251-258, 2012, [Online]. Available: https://doi.org/10.1007/s12668-012-0043-4.

[24] G. A. D. Lestari, K. D. Cahyadi, and I. E. Suprihatin, "Characterization of gold nanoparticles from clove flower water extract and its antioxidant activity," J. Sains Materi Indon., vol. 22, pp. 93-100, 2021, [Online]. Available: https://doi.org/10.17146/jsmi.2021.22.2.6644.

[25] G. B. El-Saber, L. M. Alkazmi, L. G. Wafaa, A. M. B., E. H. N., and E. K. R., "Syzygium aromaticum (Myrtaceae): Traditional uses, bioactive chemical constituents, pharmacological and toxicological activities," Biomolecules, vol. 202, pp. 1-16, 2020.

[26] C. Zaouche, A. Gahtar, S. Benramache, Y. Derouiche, M. Kharroubi, A. Belbel, C. Maghni, and L. Dahbi, "The determination of Urbach energy and optical gap energy by many methods for Zn-doped NiO thin films fabricated by spray pyrolysis," Dig. J. Nanomater. Biostruct., vol. 17, pp. 1453-1461, 2022.

[27] I. A. Abdul Hassan, "Characterizations of metals and metal oxides nanoparticles using laser ablation for biological applications," M.Sc. thesis, Univ. Wasit, Iraq, 2018.

[28] M. A. B. Muhammad, "Surface plasmon resonance-based biodetection systems: Principles, progress and applications—A comprehensive review," Biosensors, vol. 15, pp. 1-24, 2025.

[29] E. Messina, "Metal nanoparticles produced by pulsed laser ablation in liquid environment," Ph.D. thesis, Univ. of Catania, 2010.

[30] S. S. Abdullah, S. A. Salman, A. Kadhim, and A. M. Haleem, "Size control of Ag nanoparticles synthesized by PLA method in different liquid environments and their potency against virulent Candida albicans," J. Pharm. Negative Results, vol. 13, pp. 423-431, 2022.

[31] S. Dagher, Y. Haik, A. I. Ayesh, and N. Tit, "Synthesis and optical properties of colloidal CuO nanoparticles," J. Luminescence, vol. 151, pp. 149-154, 2014, [Online]. Available: https://doi.org/10.1016/j.jlumin.2014.03.018.

[32] B. H. Rabee, M. A. Habeeb, A. Hashim, and R. Mizher, "Preparation of (PVA–$AlCl_3 \cdot 6H_2O$) composites and study of optical properties," Am. J. Sci. Res., vol. 71, pp. 5-8, 2012.

[33] S. A. Ahmed and H. M. Hasan, "Silver nanoparticles synthesized by three species of genus Streptococcus and evaluation of their synergistic effects with the oil extracted from Syzygium aromaticum on some clinical bacterial isolates," Iraqi J. Sci., vol. 64, pp. 5021-5029, 2023, [Online]. Available: https://doi.org/10.24996/ijs.2023.64.12.3.

[34] O. Rodriguez, R. Sanchez, M. Verde, M. Nunez, R. Rios, and A. Chavez, "Obtaining the essential oil of Syzygium aromaticum, identification of eugenol and its effect on Streptococcus mutans," J. Oral Res., vol. 3, pp. 218-224, 2014.

[35] R. K. Bankier, Y. K. Matharu, G. G. Cheong, and E. Ren, "Synergistic antibacterial effects of metallic nanoparticle combinations," Sci. Rep., vol. 9, pp. 1607-1612, 2019, [Online]. Available: https://doi.org/10.1038/s41598-019-48243-7.

[36] M. Dhanislas, J. Joseph, P. Saundharya, G. Rajalakshmi, M. Shamya, M. Radhakrishnan, and A. Suresh, "Green synthesis of silver nanoparticles from Syzygium aromaticum and evaluation of its anti-mycobacterial activity," Acta Sci. Microbiol., vol. 6, pp. 109-117, 2023.